Journal of Harbin Engineering University
ISSN: 1006-7043

Vol 45 No. 3
March 2024

Numerical Investigation of Stress Intensity Factors for an Arc Crack in Bonded Materials Exposed to Varied Mechanical Loading Conditions

Muhammad HaziqIqmalMohdNordin[1],Khairum Bin Hamzah[2*], IskandarWaini[3], NajiyahSafwaKhashi'ie[4], Nurul Amira Zainal[5], Nik Mohd Asri Nik Long[6]

[1, 2, 3]FakultiTeknologidanKejuruteraanIndustridanPembuatan, UniversitiTeknikal Malaysia Melaka, Hang Tuah Jaya, 76100 Durian Tunggal, Melaka, Malaysia

[4,5]FakultiTeknologidanKejuruteraanMekanikal, UniversitiTeknikal Malaysia Melaka, Hang Tuah Jaya, 76100 Durian Tunggal, Melaka, Malaysia

[6] Mathematics Department, Faculty of Science, Universiti Putra Malaysia, 43400 Serdang, Selangor, Malaysia

Abstract

This study introduces fresh numerical findings that investigate an arc crack within bonded materials (BMs) positioned in the upper segment and exposed to varied mechanical loading conditions, including shear, normal, tearing, and mixed loads. This issue stems from a preceding study that exclusively focused on shear stress as a singular type of mechanical loading. Utilizing the modified complex potentials (MCPs) function, alongside smoothness constraints for the resulting force and displacement function and the crack opening displacement (COD) component as unknowns, these are formulated into hypersingular integral equations (HSIEs). The material strength associated with the arc crack is then assessed numerically by solving the HSIEs using the curve length coordinate method and Gauss quadrature procedures to determine the nondimensional stress intensity factors (NSIFs). Through graphical representations, this research vividly illustrates the significant impacts of mechanical loadings, elastic constant ratios, and geometrical parameters on the NSIFs at the crack tips. The results demonstrate that elastic constant ratios, crack geometries, and mechanical loadings collectively exert an influence on a material's strength.

Keywords:Arc crack, bonded materials, hypersingular integral equations, mechanical loading, stress intensity factors.

1. Introduction

Fracture mechanics, a discipline within engineering that explores the characteristics of solids or structures with geometric irregularities, such as the progression of cracks in materials, utilizes analytical methods from solid mechanics to compute the force acting on the crack. Concurrently, experimental approaches in solid mechanics yield measurements of materials' resistance to fracture. An integral aspect involves pinpointing critical factors known as stress intensity factors (SIFs), crucial for gauging the stress state or intensity induced by mechanical loadings or residual stresses in the vicinity of the fracture tip. Numerous researchers have addressed and examined issues related to cracks in infinite material [1, 2], half material [3, 4], or bonded materials (BMs) [5, 6]. However, all of these studies have exclusively concentrated on a single category of mechanical loading, specifically either shear or mixed stresses.

The calculation of nondimensional stress intensity factors (NSIFs) for a kinked crack originating from a hole in an infinite plate is performed through Muskhelishvili's formalism, employing the conformal mapping method [1]. The utilization of this method for a hole crack with multiple kinks demonstrates the effectiveness outlined in this paper for analyzing fatigue crack growth. A new conformal mapping is proposed in order to solve NSIFs problem in an infinite plane containing a traction-free square hole with two unequal cracks, analytically [2]. They obtained that the hole-shape had a considerable effect on the NSIFs for the small cracks though for large length cracks it is negligible. The non-hypersingular traction boundary integral equation method was employed to determine the NSIFs for a functionally graded nano-crack in a half-plane, utilizing a closed-form Green's function [3]. The investigation focused on assessing the influences of crucial problem parameters, including the size and depth of the embedded crack, surface elasticity effects, characteristics of the incident wave, and the dynamic interaction phenomenon between the crack and the free-surface boundary, on both the diffracted and scattered waves and the local stress concentration fields. The Riemann–Hilbert equation method and Cauchy integral method were utilized to present the NSIFs for a crack in an orthotropic elastic half-plane material [4]. Notably, negative Mode I NSIFs were identified for certain oblique edge crack angles and elastic constants. The flexibility of the approach is evident as the stress functions, expressed through a mapping function, enable the analysis of different geometrical shapes by simply adjusting the mapping function. The dual boundary element method was utilized to determine the NSIFs for the propagation of two-dimensional multiple cracks in BMs subjected to shear stress [5]. This investigation revealed that the SIF values were influenced by various material characteristics, affecting both the rate of crack growth and the path of fracture propagation. In a related study, the NSIFs at the tips of multiple cracks located in the top part, as well as in both the top and bottom parts of bonded materials, employing hypersingular integral equations (HSIEs) [6]. However, their focus was solely on the impact of materials susceptible to shear stress. Subsequently, they expanded their research to explore the behavior of nondimensional SIFs at the crack tips for thermally insulated cracks in bonded materials susceptible to shear stress [7]. A novel approach using a modified semi-weight function method, based on the submatrix technique, has been suggested for determining the NSIFs for cracks oriented vertically and terminating at the interface of BMs [8]. The study also delves into the influence of BMs parameters, relative crack length, and the outer integration path on the resulting NSIFs. A theoretical model of the Griffith crack in a generalized nonhomogeneous interlayer was developed by considering the influence of surface roughness of BMs and elastic properties of the adhesive material [9]. It was developed by using Cauchy integral equations and reduce to singular integral equations. The influence of elastic property and thickness of the interlayer on mode I and II NSIFs, mode mixed and energy release rate is presented through numerical results.

The focus of many researchers is often limited to a specific stress type, neglecting consideration for all mechanical loadings. As a response to this, the current numerical analysis introduces an innovative investigation into NSIFs at the crack tip of an arc crack situated in the upper part of BMs. These materials are susceptible to a range of mechanical loads, including shear, normal, tearing, and mixed loads. The outcomes of this study may offer valuable insights to engineers exploring the stability behavior of structures composed of precisely bonded materials and subjected to various mechanical loadings.

2. Mathematical Formulation

In accordance with the research conducted by Hamzah et al. [6], the normal and tangential components along the crack segment are established by the traction, revealing the hypersingular integral equations (HSIEs) for an arc crack located in the upper part of BMs, as detailed below:

$$N(t_0)+iT(t_0)=\frac{1}{\pi}\int_L \frac{g(t)\,dt}{(t-t_0)^2}+\frac{1}{2\pi}\int_L A_1(t,t_0)g(t)\,dt + \frac{1}{2\pi}\int_L A_2(t,t_0)\overline{g(t)}\,dt \tag{1}$$

where

$$A_1(t,t_0)=B_1(t,t_0)+\frac{G_2-G_1}{G_1+\kappa_1G_2}\left(\overline{B_3(t,t_0)}-\frac{d\bar{t}_0}{dt_0}\left(B_5(t,t_0)+\overline{B_4(t,t_0)}\right)+\frac{d\bar{t}}{dt}\left(B_4(t,t_0)+\overline{B_4(t,t_0)}\right)-\frac{d\bar{t}}{dt}\frac{d\bar{t}_0}{dt_0}B_6(t,t_0)\right)+\frac{\kappa_1G_2-\kappa_2G_1}{G_2+\kappa_2G_1}\frac{d\bar{t}_0}{dt_0}\overline{B_4(t,t_0)}$$

$$A_2(t,t_0)=B_2(t,t_0)+\frac{G_2-G_1}{G_1+\kappa_1G_2}\left(B_4(t,t_0)+\overline{B_4(t,t_0)}-\frac{d\bar{t}_0}{dt_0}B_6(t,t_0)+\frac{d\bar{t}}{dt}B_3(t,t_0)\right)$$

and

$$B_1(t,t_0)=\frac{1}{(t-t_0)^2}\left[\frac{(t-t_0)^2}{(\bar{t}-\bar{t}_0)^2}\frac{d\bar{t}}{dt}\frac{d\bar{t}_0}{dt_0}-1\right]$$

$$B_2(t,t_0)=\frac{t-t_0}{(\bar{t}-\bar{t}_0)^3}\left[\frac{(\bar{t}-\bar{t}_0)}{(t-t_0)}\left(\frac{d\bar{t}}{dt}+\frac{d\bar{t}_0}{dt_0}\right)-2\frac{d\bar{t}}{dt}\frac{d\bar{t}_0}{dt_0}\right]$$

$$B_3(t,t_0)=\frac{1}{(\bar{t}-t_0)^2}+\frac{2(t_0-t)}{(\bar{t}-t_0)^3}$$

$$B_4(t,t_0)=\frac{1}{(\bar{t}-t_0)^2}$$

$$B_5(t,t_0)=\frac{2(3\bar{t}_0-2t_0-\bar{t})}{(t-\bar{t}_0)^3}+\frac{6(\bar{t}_0-\bar{t})(\bar{t}_0-t_0)}{(t-\bar{t}_0)^4}$$

$$B_6(t,t_0)=\frac{1}{(t-\bar{t}_0)^2}+\frac{2(\bar{t}_0-t_0)}{(t-\bar{t}_0)^3}.$$

Please note that in this given context, "*t*" and "t_0" represent specific values along the crack, where "*g(t)*" is crack opening displacement function, "*G*" represents the shear modulus of elasticity, "$\kappa=(3-v)/(1+v)$" pertains to plane stress, "$\kappa=3-4v$" to plane strain, and "*v*" denotes Poisson's ratio. Subscripts "1" and "2" distinguish between the top and bottom sections, respectively, and an overline on a function indicates its conjugated value. It is essential to keep in mind that the hypersingular integral is denoted by the initial integral in Eq. (1) and must be specified as a finite part integral.

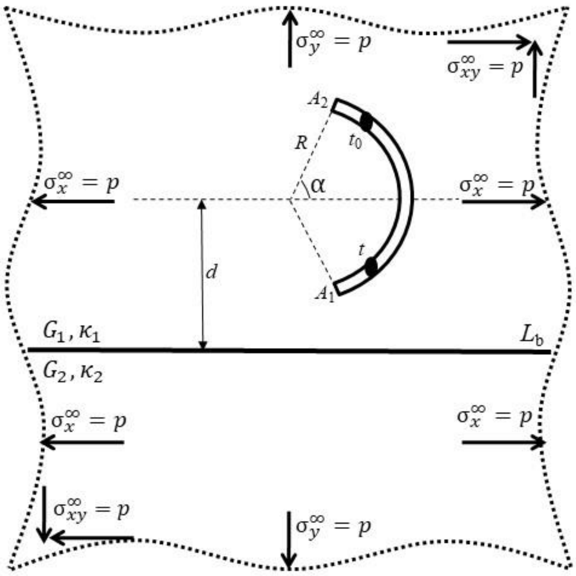

Fig. 1. An arc crack in BMs exposed to varied mechanical loading conditions

Consider the geometry conditions for an arc crack that exists in the top part of BMs exposed to varied mechanical loading conditions such as shear $\sigma_x^\infty = p$, normal $\sigma_y^\infty = p$, tearing $\sigma_{xy}^\infty = p$, and mixed $\sigma_x^\infty=\sigma_y^\infty = p$ loads as shown in Fig. 1. Note that, *d* is the distance between the crack and the boundary L_b. In order to calculate the nondimensional SIFs, we need to include the types of mechanical loading in the crack problems. For shear load, the condition of the normal and tangential component with an angle of the crack α is defined as follows [10]

$$\frac{1}{E_1}\sigma_{x_1}=\frac{1}{E_2}\sigma_{x_2},\quad N+iT=-p\sin^2\alpha-ip\sin\alpha\cos\alpha \tag{3}$$

for normal load is defined as follows

$$\frac{1}{E_1}\sigma_{y_1}=\frac{1}{E_2}\sigma_{y_2},\quad N+iT=-p\cos^2\alpha+ip\sin\alpha\cos\alpha \tag{4}$$

for tearing load is defined as follows

$$\frac{1+\tau_1}{E_1}\sigma_{x_1y_1}=\frac{1+\tau_2}{E_2}\sigma_{x_2y_2},$$
$$N+iT=2p\sin\alpha\cos\alpha+ip\left(\cos^2\alpha-\sin^2\alpha\right) \tag{5}$$

whereas mixed load is defined as follows

$$\frac{1-\tau_1}{E_1}\sigma_{x_1}=\frac{1-\tau_2}{E_2}\sigma_{x_2},\quad N+iT=-p+i0 \tag{6}$$

where $E_j=2G_j(1+\tau_j)$ and $j=1,2$ are Young's modulus of elasticity for top and bottom parts of bonded materials.

3. Results and Discussion

As presented in Fig. 1, consider the geometrical conditions for an arc crack that exists in the top part of BMs exposed to varied mechanical loading conditions such as shear, normal, tearing, and mixed loads when $d=1.5R$ and α varies at all crack tips.

Fig. 2 presents the graphical results for the NSIFs F_1 and F_2 for an arc crack in BMs exposed to shear load at all crack tips. It is obtained that as α increases F_1 decreases at all crack tips and F_2 does not show big changes. Whereas as G_2/G_1 increases F_1 decreases but F_2 increases at all crack tips. The numerical outcomes present indications that an increase in α

and G_2/G_1 leads to greater stability in the materials strength.

Fig. 3 presents the graphical results for the NSIFs F_1 and F_2 for an arc crack in BMs exposed to normal load at all crack tips. It is obtained that as α increases F_1 does not show big changes at all crack tips and F_2 decreases at tip A_1 but increases at tip A_2. Whereas as G_2/G_1 increases both F_1 and F_2 increases at tip A_1 but decreases at tip A_2. The numerical outcomes present indications that the materials strength depends on the value of α and G_2/G_1.

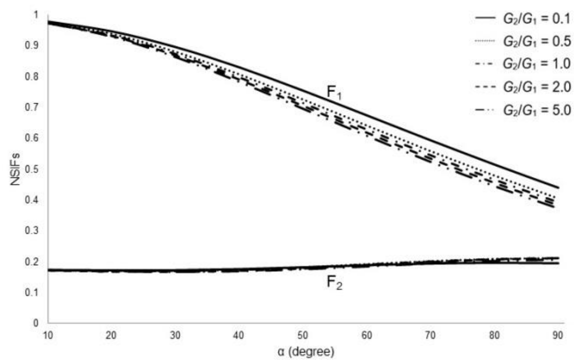

(a) at tip A_1

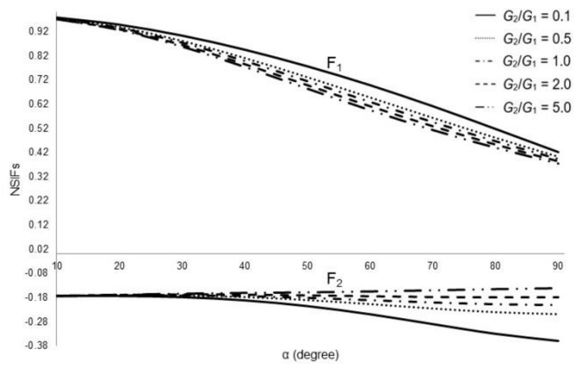

(b) at tip A_2

Fig. 2. NSIFs for an arc crack in BMs exposed to shear load

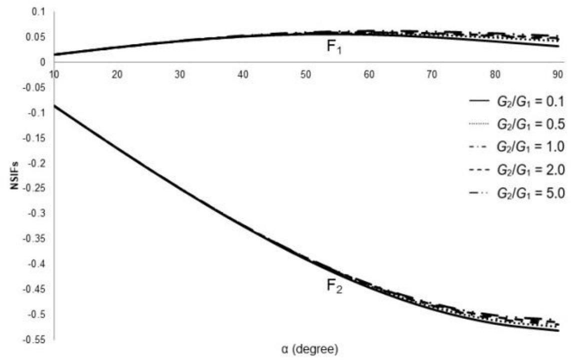

(a) at tip A_1

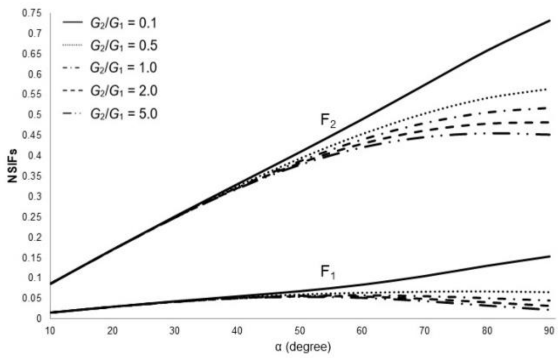

(b) at tip A_2

Fig. 3. NSIFs for an arc crack in BMs exposed to normal load

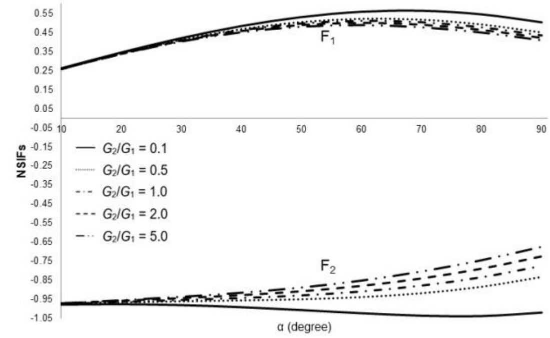

(a) at tip A_1

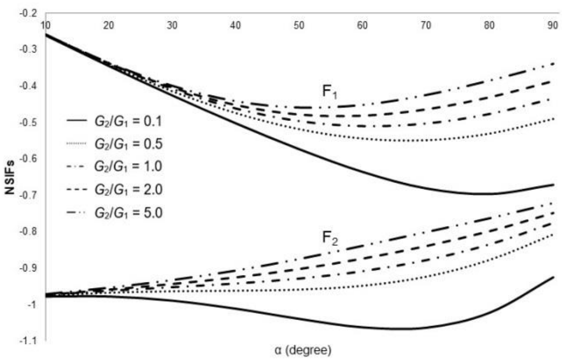

(b) at tip A_2

Fig. 4. NSIFs for an arc crack in BMs exposed to tearing load

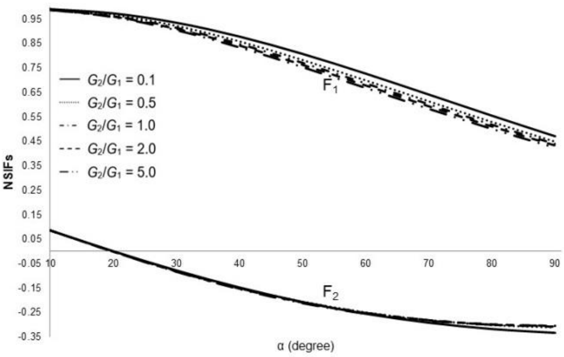

(a) at tip A_1

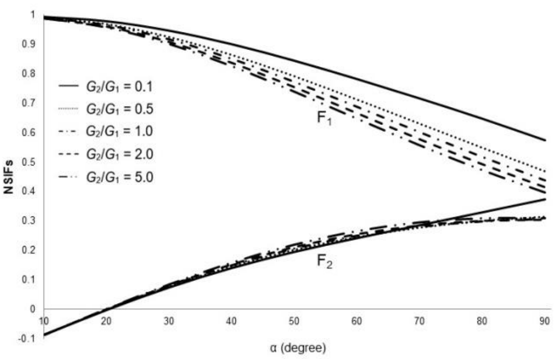

(b) at tip A_2

Fig. 5. NSIFs for an arc crack in BMs exposed to mixed load

Fig. 4 presents the graphical results for the NSIFs F_1 and F_2 for an arc crack in BMs exposed to tearing load at all crack tips. It is obtained that as α increases F_1 increases at crack tip A_1 but decreases at tip A_2, and F_2 increases at al crack tips. Whereas as G_2/G_1 increases F_1 decreases at crack tip A_1 but increases at tip A_2, and F_2 increases at all crack tips. The numerical outcomes present indications that an increase in α results in a reduction in the materials' strength, whereas an increase in G_2/G_1 leads to greater stability in the materials strength.

Fig. 5 presents the graphical results for the NSIFs F_1 and F_2 for an arc crack in BMs exposed to mixed load at all crack tips. It is obtained that as α increases F_1 decreases at crack tips, and F_2 decreases at crack tip A_1 but increases at tip A_2. Whereas as G_2/G_1 increases F_1 decreases at all crack tips, and F_2 increases at all crack tips. The numerical outcomes present indications that an increase in α and G_2/G_1 leads to greater stability in the materials strength.

4. Conclusion

This research is specifically centered on numerically investigating NSIFs at the tips of an arc crack in the upper region of BMs, which is exposed to various mechanical loadings such as shear, normal, tearing, and mixed loads. Unlike previous studies that focused solely on shear stress, our investigation spans different types of mechanical loadings. The modified complex potential function is utilized to HSIEs for the model, with the COD function serving as the unknown and incorporating continuity conditions for resulting force and displacement. Through numerical graphical representation, this study highlights the significant influence of mechanical loadings, the elastic constant ratio, and the geometrical conditions of the crack on NSIFs. The following key observations help elucidate the main findings of the analysis:

The strength of materials for an arc crack in the upper part of BMs is dependent on the elastic constant ratio, the types of mechanical loadings applied, and the geometric conditions of the crack.

Prospective investigations could expand upon the methodology utilized in this study to explore the behavior of NSIFs across different geometric scenarios, particularly in situations involving multiple cracks within BMs undergoing varied mechanical loading. Leveraging insights from Chen and Lee [11], this approach may also be adapted for addressing challenges associated with three-dimensional cracks in bonded materials.

Acknowledgement

The correspondingauthorwouldlike to thank the Ministry of Higher Education (Malaysia) through the grants: FRGS/1/2021/STG06/UTEM/03/2 and UniversitiTeknikal Malaysia Melaka (UTeM) for financial support.

References

[1] Li, Y. and Zheng, K., 2021. Stress intensity factor analysis of kinked and hole crack in an infinite plate using numerical conformal mapping. Theoretical and Applied Fracture Mechanics, 114, p.103022.

[2] Ghajar, R. and Hajimohamadi, M., 2019. Analytical calculation of stress intensity factors for cracks emanating from a quasi-square hole in an infinite plane. Theoretical and Applied Fracture Mechanics, 99, pp.71-78.

[3] Rangelov, T.V., Dineva, P.S. and Manolis, G.D., 2020. BIEM analysis of a graded nano-cracked elastic half-plane under time-harmonic waves. ZAMM-Journal of Applied Mathematics and Mechanics/ZeitschriftfürAngewandteMathematik und Mechanik, 100(6), p.e202000021.

[4] Hasebe, N., 2021. Stress analysis for an orthotropic elastic half plane with an oblique edge crack and stress intensity factors. ActaMechanica, 232, pp.967-982.

[5] e Andrade, H.D.C. and Leonel, E.D., 2019. The multiple fatigue crack propagation modelling in nonhomogeneous structures using the DBEM.

Engineering Analysis with Boundary Elements, 98, pp.296-309.

[6] Hamzah, K., Nik Long, N.M.A., Senu, N. and Eshkuvatov, Z., 2020. Stress Intensity Factors for Crack Problems in Bonded Dissimilar Materials. Journal of Engineering & Technological Sciences, 52(5).

[7] Hamzah, K.B., Long, N.N., Senu, N. and Eshkuvatov, Z.K., 2021. Numerical solution for the thermally insulated cracks in bonded dissimilar materials using hypersingular integral equations. Applied Mathematical Modelling, 91, pp.358-373.

[8] Huang, D.Y., Rao, Q.H., Ma, Y., Yi, W. and Shen, Q.Q., 2021. A modified semi-weight function method for stress intensity factor calculation of a vertical crack terminating at the interface. Theoretical and Applied Fracture Mechanics, 116, p.103107.

[9] Zhang, A.B., Lou, J., Wang, B. and Wang, J., 2023. A Griffith crack model in a generalized nonhomogeneous interlayer of bonded dissimilar half-planes. J. Theort. Appl. Mech, 61, pp.495-507.

[10] Chen, Y.Z., Hasabe, N. and Lee, K.Y., 2003. Multiple crack problems in elasticity. WIT Press, Southampton, Boston.

[11] Chen, Y.Z. and Lee, K.Y., 2001. Numerical solution of three-dimensional crack problem by using hypersingular integral equation. Computer methods in applied mechanics and engineering, 190(31), pp.4019-4026.